Medical Engineering and Physics 69 (2019) 8–16

Contents lists available at ScienceDirect

Medical Engineering and Physics

journal homepage: www.elsevier.com/locate/medengphy

A general multi-objective topology optimization methodology developed for customized design of pelvic prostheses

Taimoor Iqbal[a,b], Ling Wang[a,b,*], Dichen Li[a,b], Enchun Dong[a,b], Hongbin Fan[c], Jun Fu[c], Cai Hu[d]

[a] State Key Laboratory for Manufacturing System Engineering, Xi'an Jiaotong University, Xi'an, Shaanxi 710054, PR China
[b] School of Mechanical Engineering, Xi'an Jiaotong University, Xi'an, 710054, PR China
[c] Department of Orthopedics, Xijing Hospital, Air Force Medical University, Xi'an 710032, PR China
[d] Shaanxi Institute of Medical Device Quality Supervision and Inspection, Xi'an 712046, PR China

ARTICLE INFO

Article history:
Received 21 November 2018
Revised 29 May 2019
Accepted 10 June 2019

Keywords:
Topology optimization
Customized design of pelvic replacements
Finite element analysis
Multi-activities
Additive manufacturing

ABSTRACT

In this study, a multi-objective topology optimization method has been formulated and carried out for various resection types, with minimization of a weighted sum of the compliance (maximized stiffness) under six routine activities of daily life as the objective function and volume reduction as a constraint. Unique prosthetic geometries with low weight and remarkable strength closely matching the pelvic bone shape were obtained. The strength of the optimized implants was investigated through finite element analysis and it has been found that the initial geometries of the optimized implants could withstand the static loading conditions of various routine activities having less stress concentration areas. A 3D printed patient-specific topology optimized hemi-pelvic prosthesis has been designed based on the proposed method and implanted successfully in a patient with pelvic sarcoma. Therefore, pelvic prostheses can be designed and then manufactured via additive manufacturing technologies with the minimum material in less time and having robust mechanical fixation responses. Conclusively, the topology optimization method used for the design of pelvic prostheses improves the biomechanical performance of the implants with reduced weight and higher stiffness than the traditional implants. Including the topology optimization procedure in the phase of designing patient-specific pelvic implants is therefore, highly recommended.

1. Introduction

Along with the protection of pelvic contents and muscle attachments, the major functions of the pelvic bone are to provide continuity and to transfer loads between the lower extremities and the central skeleton by means of articulations at the hip joint and sacroiliac joints [1]. An outspread tumor at the pelvis can necessitate a resection, which requires a custom implant for the reconstruction of the pelvis. Resections of the pelvis are classified into three main types, according to the location of the defect [2]: type I involves resection of the ilium, type II involves the resection of the periacetabular region, and type III of the ischium and pubic rami portions. Patients with a primary malignant periacetabular sarcoma involving the sacroiliac joint will require an en bloc resection of the acetabulum and ilium [3]. This type of resection is classified as type I+II. Similarly, type II+III contains the resection of the acetabulum and obturator foramen, as shown in Fig. 1.

Existing pelvic prostheses were usually designed using either reverse engineering methods or an oversimplified beam section. The former involves overly complex geometry, which leads to long manufacturing times and surgical complications; the latter might be oversimplified in terms of strength and stability [4,5]. Both are based on theoretical support in terms of strength and safety. Moreover, there is a minimal selection of commercially available standard prostheses, owing to the high demands of geometrical adaptiveness. Previously designed hemi-pelvic prostheses, for example, saddle prosthesis is not recommended for the pelvic reconstruction after the tumor resection due to its increasing mechanical failure rates [6]. The designs of saddle prosthesis and ice-cream cone prosthesis are unable to rebuild the pelvic ring structure which can subsequently result in implant loosening and can be a reason for morbidity [7,8]. Although the modular prosthesis can rebuild the pelvic structure well [3], the complicated prosthetic components may rise the surgical complications and

* Corresponding author at: State Key Laboratory for Manufacturing Systems Engineering, Xi'an Jiaotong University, Xi'an, Shaanxi 710054, China.
E-mail address: menlwang@xjtu.edu.cn (L. Wang).

https://doi.org/10.1016/j.medengphy.2019.06.008
1350-4533/

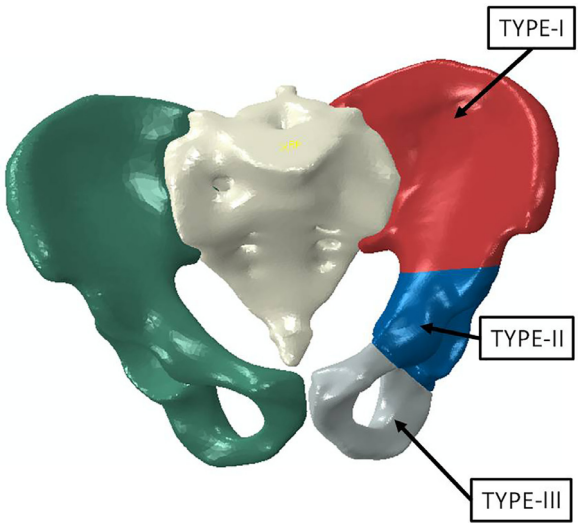

Fig. 1. Anatomy of the human pelvis with three basic resection types.

subsequently instability of the implant [9]. Prostheses designed for heavy load bearing regions are normally made from alloy metals such as cobalt-chromium alloys, titanium-based alloys, 316L stainless steel, and tantalum [10]; hence, they can be significantly heavier than the replaced bone. Moreover, the increased weight of a prosthesis can place a strain on the pelvis and can increase mechanical energy expenditure and muscular effort at the hip [11]. Therefore, a custom design with optimized mechanical *in-situ* performance and minimized volume and weight becomes necessary.

Topology optimization (TO) is a design method that proposes an optimal material layout with maximum stiffness and minimum volume/weight constraints under given loading and boundary conditions [12]. TO integrated with the finite element (FE) method can be used to optimize the implant material to satisfy particular requirements [13]. This can be achieved by eliminating the material from the region associated with the lowest von Mises stress while retaining the regions of high stress [14]. These topology-optimized implants may have a complex geometry. Additive manufacturing (AM) or 3D printing techniques can fabricate complex geometries that cannot be created by conventional manufacturing methods [15]. The main advantages of a topology optimized custom prosthesis are (1) low cost of material and manufacturing, (2) opportunities to reduce stress shielding [16], (3) smaller incisions, (4) implant can be placed in the optimal position for better ingrowth of bones, and (5) ensured mechanical functionality.

TO has been applied to the design of new layouts with optimized material allocation in the industry [17,18], and has been used for the customization of bone implants, particularly dental [19–21], spine [22,23] and hip implants [10,13,16,24–29]. However, to the best of our knowledge, it has not been applied to the design of pelvic prostheses. Therefore, this is a novel work presenting the optimization for the design of patient-specific pelvic prostheses for various resection types.

This study aims to optimize the design of pelvic replacements for different resection types by using topological optimization, thereby, achieving the best performance with respect to sizes, strength, and long-term stability of the prosthesis. A TO method is developed and generalized to obtain the optimal geometry of a hemi-pelvic prosthesis for pelvic reconstructions involving type I, II, I&II, and II&III resections. The strength and feasibility of the optimized implants were also inspected through the simulations of the most strenuous routine activities.

2. Materials and methods

2.1. Finite element model of the natural human pelvis

This FE model is based on the CT (Computer Tomography) data of a male patient (64-year-old, weight 68 Kg, height 1.68 m) [30]. The CT data was imported in the form of DICOM into Mimics software (16.0, Materialise Inc., Leuven, Belgium) and the related tools were used to construct triangle based surface models of the pelvis. The right hemi-pelvis was mirrored to the left affected side of the pelvis. The parameters of these surface meshes were optimized in 3-matic (8.0, Materialise Inc., Leuven, Belgium) and Geomagic Studio (12, Geomagic, USA) and then converted into 4-node linear tetrahedron elements (C3D4) using Hypermesh (14.0, Altair Engineering Inc., USA).

Inhomogeneous material properties were rendered to the pelvic model according to the corresponding grey scale value. Overall 10 levels of material properties were automatically assigned onto the bone model in Mimics, by using a uniform method for realistic material assignment based on the following relations [31] between Hounsfield units(H.U), ρ_B(bone density) and E (elastic modulus).

$$\rho_B = 6.9141exp - 4 \times \text{H.U} + 1.026716 \quad (1)$$

$$E = 2017.3 \times \rho_B exp2.46 \quad (2)$$

Hence, the assigned Young's Modulus of left hemi-pelvis, sacrum, and right hemi pelvis ranged from 2.02 to 10.23 GPa, 1.83 to 9.67 GPa and 2.02 to 10.02 GPa respectively, whereas the Poisson's ratio was set to be 0.3 for the whole pelvic bone. The femoral head was modeled as a rigid body using a solid sphere with reference to the patient's data. Tie (bonded) contact pair was used to define interfacing surfaces between the femoral head and acetabulum. For simplification purposes, the effects of the ligaments were neglected in the FE model.

2.1.1. Load and boundary conditions

The coordinate system of the pelvis was defined as: the x-axis runs through the centers of femoral heads from right to left, the y-axis was perpendicular to the anterior plane and z-axis was perpendicular to both x- and y-axes (Fig. 2(a)). Centre of mass (COM) (a point where the entire mass of the object is concentrated and the object can be balanced at this point) of the pelvis was obtained by using the mass properties in Abaqus(6.14, Abaqus Inc., USA) and origin was set at this COM. Resultant of peak contact forces for the six most occurring activities was obtained from the literature [32], normalized according to the body weight (BW) of the patient and summarized in Table 1 with the number of cycles per year of each activity. Nodes on the sacrum S1 superior surface were fully constrained for all degree of freedom (DOF), and the component loads were applied through the spherical centers of both femoral heads (Fig. 2(a)). Each load case was simulated as static explicit using Abaqus (6.14, Abaqus Inc., USA).

2.1.2. Model verification and validation

Mesh refinement tests were conducted to verify the model until a change of less than 5% in the peak values of Von Mises Stress was obtained. The model was validated by being compared with the fixed boundary condition model of ATM Phillips [33] for single leg standing, and similar stress-strain patterns were observed.

2.2. Topology optimization

The aims of applying the TO on design of the pelvic prosthesis is to reduce the weight/volume of the prosthesis by removing the unnecessary material from the region with zero loading to bear

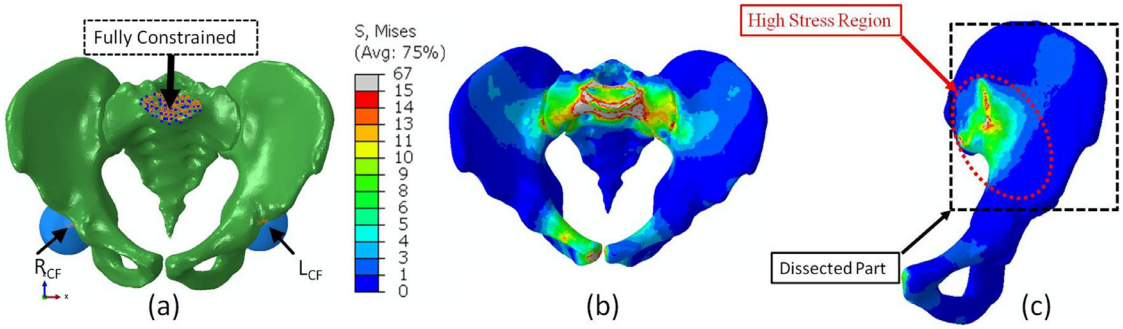

Fig. 2. (a) Finite element model setup of the natural human pelvis for multiple activities (b) von Mises stress distribution in the healthy pelvis during standing up, and (c) von Mises stress distribution in left hemi-pelvis during standing up for volume estimation.

Table 1
Summary of the hip contact forces and the annual occurrence frequencies for routine activities.

#	Activity		Fx(N)	Fy (N)	Fz(N)	Number of cycles per year (Normal patient)(×1000)
1	Normal walking	R_{CF}	325.45	−39.26	446.75	1369.3
		L_{CF}	−230.18	−164.39	1495.24	
2	Single leg standing	R_{CF}	−136.1	21.71	131.71	63.5
		L_{CF}	−296.04	−61.26	1186.6	
3	Standing up	R_{CF}	524.09	804.7	621.62	20.1
		L_{CF}	−524.09	804.7	621.62	
4	Sitting down	R_{CF}	497.68	−675.49	418.19	20.1
		L_{CF}	−497.68	−675.49	418.19	
5	Stair ascending	R_{CF}	340.19	−15.79	650.41	41.4
		L_{CF}	−117.98	552.56	1613.16	
6	Stair descending	R_{CF}	177.43	−1.72	427.75	41.4
		L_{CF}	−288.89	−615.66	1666.47	

R_{CF} and L_{CF} refer to the right and left centers of femoral heeds respectively.

when the pelvis is under the loading conditions of the six most frequent daily activities, as well as to guarantee the strength and stability of the prosthesis when under physiological mechanical environment.

To accomplish the goal, a multi-objective TO formulation has been set up with the minimization of weighted sum of the strain energy (i.e. maximize the stiffness) due to six most frequent daily activities as the objective function, while constraining the volume fraction. Density is taken as a design variable, whose values range from 0 (void) to 1 (solid). Based on the work of Sigmund [34] and Bendsøe and Sigmund [35], the mathematical formulation of TO is expressed as follows:

Objective function:

$$Min\left(C=\sum_{n=1}^{6}W_n.C_n\right),\ 0<W_n<1,\ \sum_{n=1}^{6}W_n=1 \tag{3}$$

Where C is compliance of the region to be optimized and W_n is the weighing factor for each load case calculated based on the number of cycles per year i.e.

$$W_n=\frac{Number\ of\ cycles\ (per\ year)of\ activity\ n}{\sum_{n=1}^{6}(cycles\ per\ years)} \tag{4}$$

Constraints:

$$V(\rho)=\int_{\Omega}\rho dV\le V_{max} \tag{5}$$

$$0<\rho_{min}\le\rho_e\le 1 \tag{6}$$

Where ρ is the density vector, $\rho_{min}(=0.001)$ and ρ_e are the minimum relative density and the relative density of element e respectively. V is the volume to be computed, which is a function of density (ρ), whereas V_{max} is the volume constraint.

Instead of using an irregular shape pelvic bone part, the proposed (dissected) area has been replaced by a regularly shaped box as an initial structure (often referred to as the design domain or design space) surrounding the affected part on which the TO has been applied. To maintain the special features of the bone, Boolean operations were used to ensure that contact could be accomplished within the remaining pelvic bones. The regions of the interface between bone and implant were modeled as tied (bonded) and considered "frozen" during the TO process which warrants that no material will be removed during the process, so that attachment location could be determined (Fig. 3).

The material properties of titanium alloy (Ti6Al4V) ($E=110$ GPa, $\nu=0.3$) were assigned in Abaqus to the design domain after meshing in Hypermesh with C3D4 elements. The models for TO have been configured with the same load and boundary conditions as that of the natural pelvic model. The Solid Isotropic Material with Penalization (SIMP) [35,36], -based general optimization technique has been applied through the Abaqus Topology Optimization Module (ATOM) to simulate the TO process with a penalization factor $P(=3)$.

The volume of design domain for resection types I, II, I+II and II+III have been constrained to 5%, 7%, 3%, and 3% respectively by comparing the volumes of the design domain and the effective stress region that can be subjected to material retention during the TO process (Fig. 2(c)). The optimization results were extracted and saved as STL files. These STL files were exported into 3-matic software and discrete geometries were created using split surfaces. Once the design was achieved, the geometries were remeshed in Hypermesh as a solid (C3D4), and FEA of the reconstructed pelvis with optimized implants under the load and boundary conditions similar to the natural human pelvis model was performed to determine the strength of prostheses and their effects on the pelvic bone.

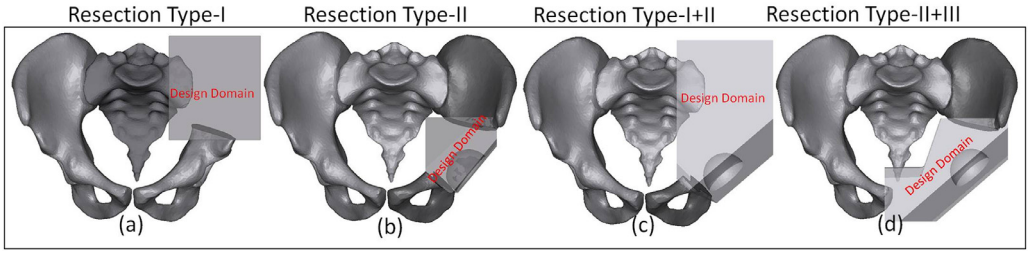

Fig. 3. Design domains for various resection types.

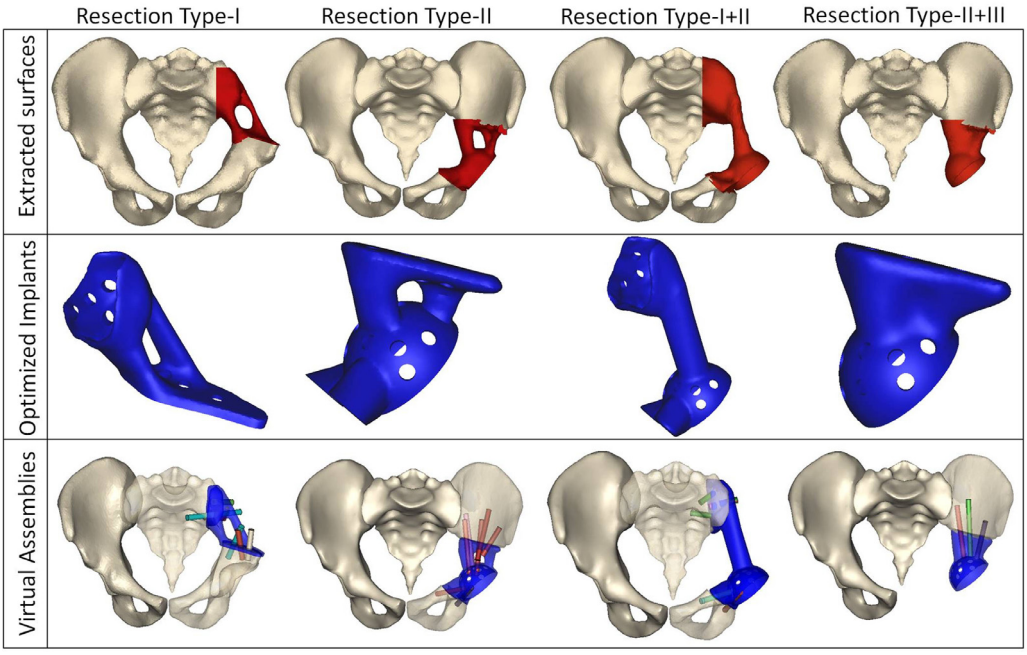

Fig. 4. Topology-optimized extracted surfaces, Optimized implants and virtual assemblies with topology-optimized implants.

3. Results

3.1. Topology optimization output

Four patient-specific pelvic prostheses designs were achieved based on the TO results. Consequently, unique optimum designs with reduced volumes of 19%, 31%, 18% and 22% of the corresponding dissected parts were obtained for optimized implants of resection types I, II, I+II, and II+III respectively (Fig. 4).

3.2. FEA results with optimized implants

The results presented here are only for the activity having maximum stress values (the worst case) among all six activities.

3.2.1. von Mises stresses in optimized implants and pelvic bone

The distributions of the von Mises stress observed in the optimized implants are illustrated in Fig. 5. Peak von Mises stress value of 74 MPa was observed at the supporting rod in the type-I prosthesis (Fig. 5(a)) during standing up activity. In the type-II prosthesis, the maximum value of von Mises stress of 126 MPa was seen at the rim of the acetabulum cup during ascending stairs (Fig. 5(b)). The peak von Mises stress of 91 MPa was recorded in the type-I+II implant during standing up at the connecting rod near the left sacroiliac joint (Fig. 5(c)). For the type-II+III prosthetic component maximum von Mises stress of 112 MPa was observed at the bone-implant interface during stair descending (Fig. 5(d)). Peak values of von Mises stress during all six activities in the reconstructed pelvic bone and optimized implants for each resection type are shown in Fig. 6.

3.2.2. Shear stresses in optimized implants

Shear stress distributions for optimized implants during the activities with maximum stress are shown in Fig. 7. For type-I and type-II+III a small region is under the maximum shear stress at the implant-bone interface on left ilium. Whereas peak shear stresses in type-I+II prosthesis can be seen at the implant-bone interface on the left sacroiliac joint. In type-II prosthesis, a little part of the rim of cup bears maximum shear.

3.2.3. Principal stresses in natural and reconstructed pelvic bone

The maximum principal stress distributions in the natural and reconstructed pelvic bones are shown in Fig. 8. It can be seen that after resection type-I and I+II, during standing up activity (Fig. 8 (d, f)) the pelvic bones mostly bear tension stress, whereas for the resection type-II and II+III, during ascending and descending stairs (Fig. 8(e, g)) respectively, the pelvic bones mainly bear compressive stresses. The peak tensile stress has been observed only at the articular surfaces of left and right sacroiliac joints and at the surface of the S1 due to fixed boundary conditions.

4. Discussions

A multi-objective TO method was established for the designing of hemi-pelvic prostheses having maximum strength with minimum weight/volume under the physiological loadings conditions

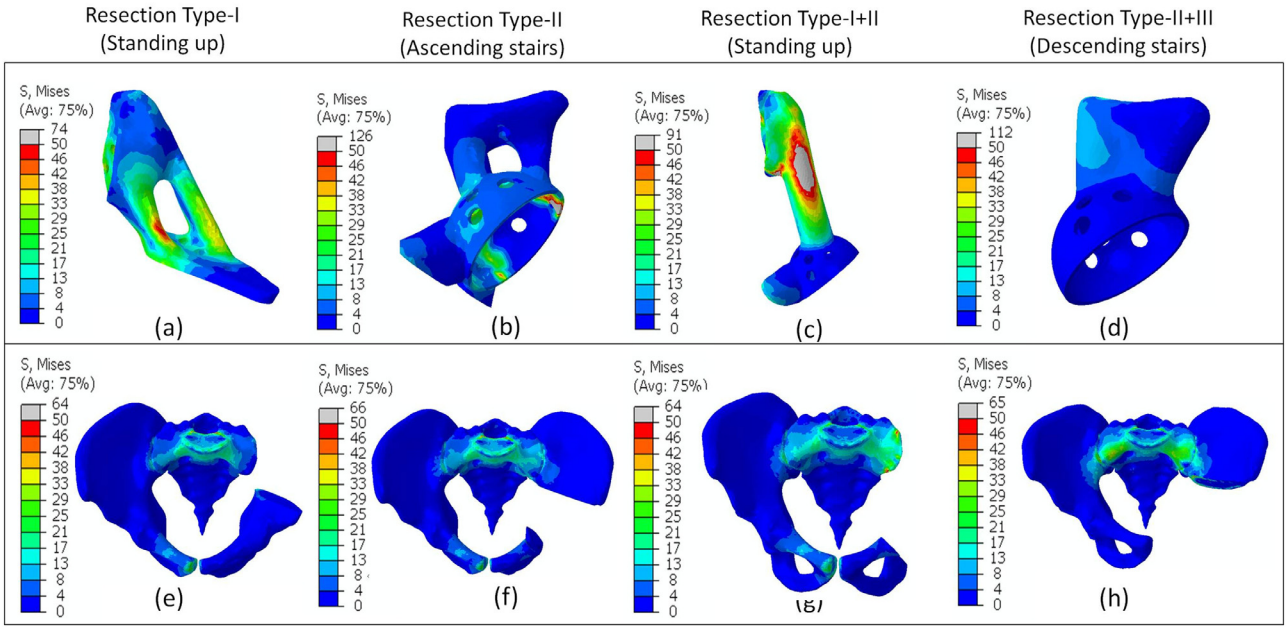

Fig. 5. von Mises stress distributions in (a–d) optimized implants and (e–h) reconstructed pelvic bone during the activities with maximum stress values.

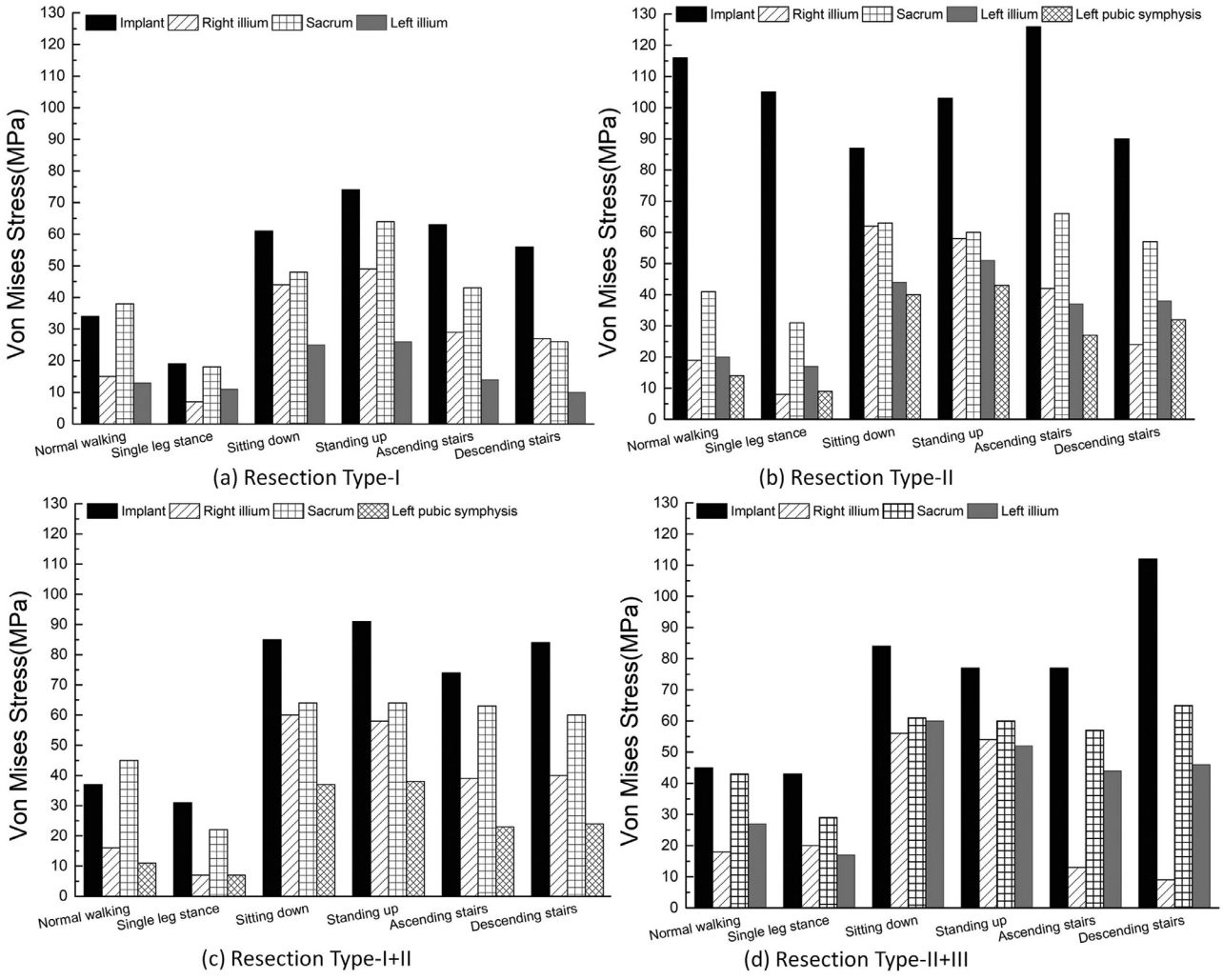

Fig. 6. von Mises stress distributions in optimized implants and reconstructed pelvic bone during all routine activities for each resection type.

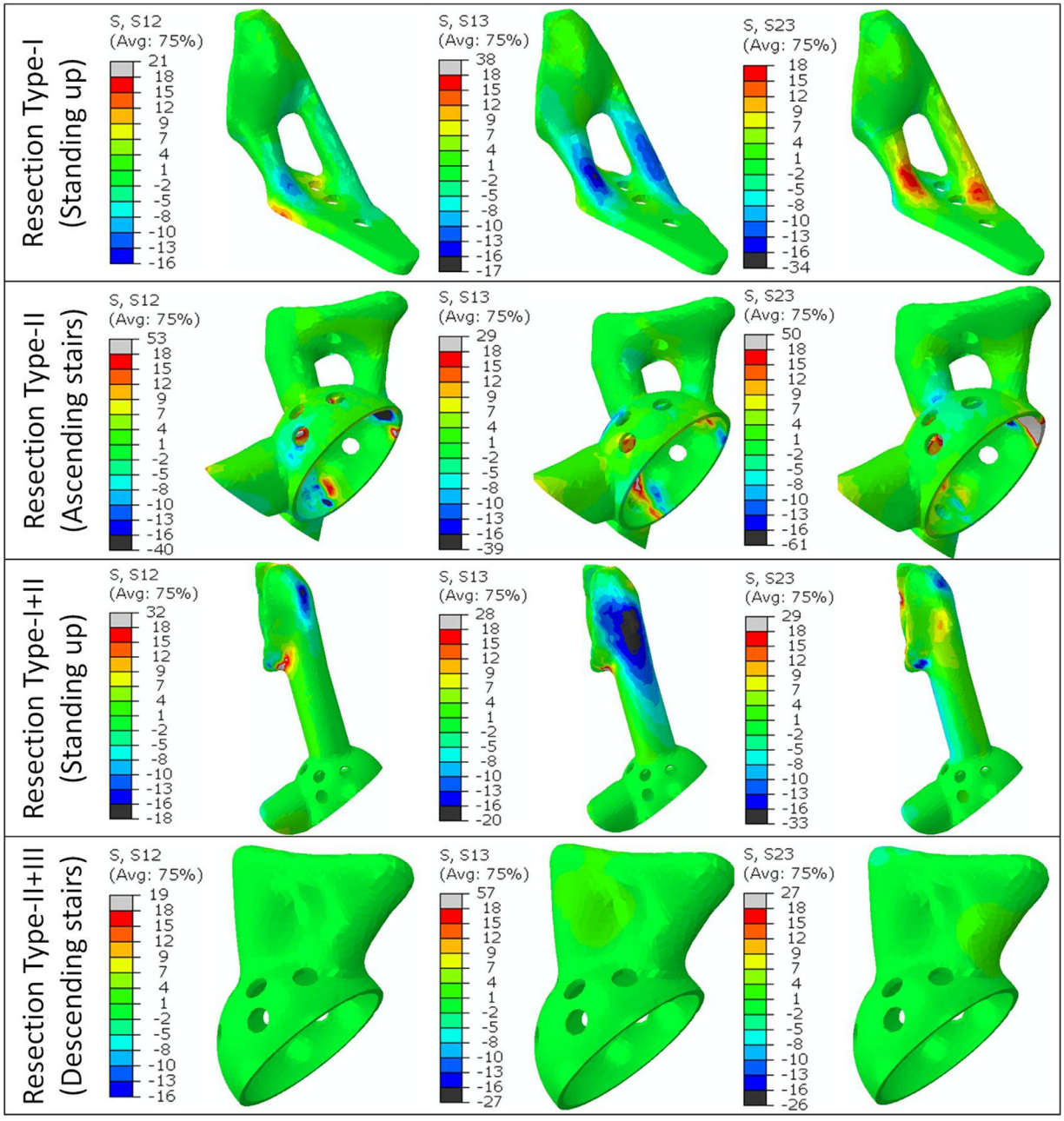

Fig. 7. Shear stresses in optimized implants ($S_{12} = \tau_{xy}, S_{13} = \tau_{xz}, S_{23} = \tau_{yz}$).

of various routine activities. The generality of the proposed technique has been demonstrated and vivificated after being applied to various pelvic resection types. In addition, along with the customization of patient-specific implant tailoring in respect of the connecting interface and fixation system design, this optimization method is expected to provide a general way to design personalized pelvic prostheses with significantly reduced weight/volume and improved functionality.

Due to their complicated design components and manufacturing process, long-term preoperative planning is required for most of the previous custom-designed hemi-pelvic prostheses. The TO methodology presented in this study for the design of hemi-pelvic prostheses for various resection types can accelerate the surgical planning. Moreover, the prostheses designed by the TO process are exactly matched to the individual patient's anatomy. Also, the fixation points can be defined at an early stage of the design and perfectly positioned according to the requirements of the surgery. This can, in turn, help to maintain the pelvic bone functionality and reduce the implant loosening. Most of the standard and custom-designed pelvic prostheses reported in the literature [3,4,9,37,38] were designed for a specific resection type and/or for a particular pelvic replacement. However, the TO based designing method presented in this study can be applied to various resection types. Moreover, this method can be extended to any other pelvic replacement according to the need of the patient.

Both the directions and magnitudes of the forces at hip joint varies along with different instant of the normal daily activities as reported from the literature [32]. In addition, TO result is sensitive to the loading direction rather than to the load magnitude. Hence, for the design of pelvic bone replacement prosthesis, it is critical to consider the strength of the prosthesis under all scenarios of loading environment corresponding to various routine

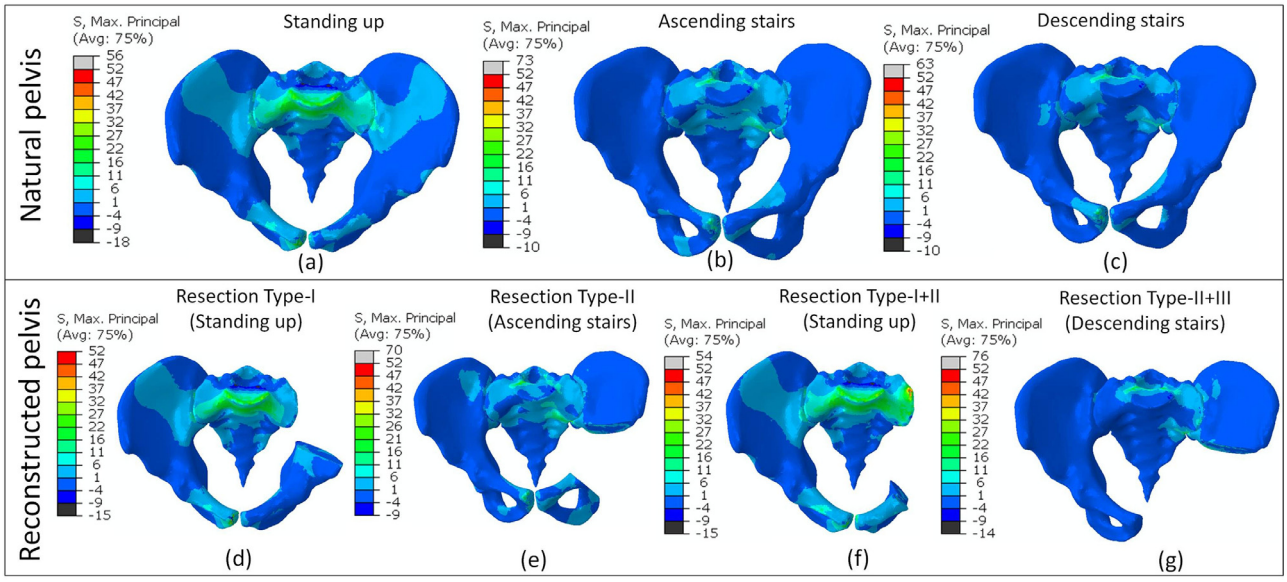

Fig. 8. Principal stress distributions in (a–c) natural pelvic bone and (d–g) reconstructed pelvic bone.

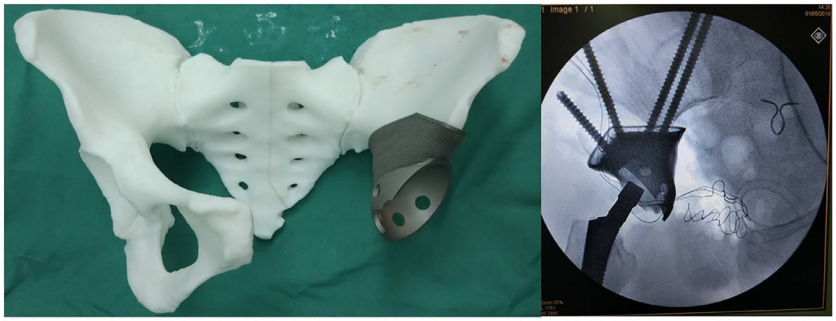

Fig. 9. (a) 3D printed prosthesis in a demo pelvis before implantation and (b) the radiographic image of the prosthesis after implantation.

activities. Therefore, six types of the most recurring and strenuous routine activities were incorporated in one single TO through a multi-objective formulation. To achieve this goal, an individual weighting factor was determined for each daily activity based on the occurrence frequency of each activity and utilized in the objective function of the TO.

To overcome the convergence difficulties of the TO process due to the irregular and complex shape of the pelvic model, a regular shaped box surrounding the resected part has been proposed as the design domain. Some authors [20,39] used measurement tools to find the dimensions of the defects and then generate the design space, which can be complicated and time-consuming. This method provided a more flexible and straightforward way to perform the TO process. By using such a method, novel prosthetic geometries based on the proposed solution of TO have been designed corresponding to various resections.

The strength of optimized implants and their effects on the host tissue have been determined via FEA. No stress concentrations have been seen at the implant-bone interfaces in all cases except type-II+III prosthesis, however, the stress values are below the threshold to affect the stability. Stress distribution patterns in the reconstructed pelvis with the optimized prostheses show good resemblance with the load transfer path reported by Neumann [40]. This indicated that the optimized prostheses have the potential to restore the biomechanical function of the pelvic ring after resections under the loading conditions of the six most strenuous routine activities. The peak values of von Mises stress (Fig. 6) in the reconstructed pelvic bone and optimized prostheses are well below the yield strength of the cortical bone (150 MPa) [41] and additively manufactured Ti6Al4V (822–1188 MPa) [42,43]. Thus, the strength of the designed prostheses has been proved to fulfill the requirement of all daily activities. High shear stresses can be observed at the bone-implant interface in type-I and II+III resections, mainly caused by the tie (bonded) interface set up, indicating the potential risk of osteoporosis and implant loosening. Therefore, special treatment such as porous structural biomaterials design or coating with some biocompatible materials is necessary at such region. Moreover, the inclusion of screws for fixation might lower the shear stresses at the implant-bone interface that would be studied in future work.

The distribution of the principal stress vectors during the descending stairs activity before and after the resection type-II+III (Fig. 8(c, g)) suggests that stress shielding phenomenon is not prone to occur after the replacement of type-II+III optimized implant. However, a slight decrease in the compressive and tensile stress values on the pelvic bone after resection types-I, II and I+II, when compared to those of the natural pelvic bone, indicates potential stress shielding. Nevertheless, overall similarities in the principal stress distributions in both natural pelvic bone (Fig. 8(a–c)) and in the reconstructed pelvic bone (Fig. 8(d–g)) manifest that the bone morphology may not change much after replacement of implant and the bone can remodel in accordance

with the Wolff's law [44], which in turn may ensure long-term stability of the implants.

A hemi-pelvic prosthesis has been designed by using the proposed TO method for the resection type II+III for a patient with a pelvic bone tumor. This implant was fabricated using Electron Beam Melting (EBM) technology in Ti6Al4V and successfully implanted at Xijing Hospital Xi'an, China (Fig. 9) about nine months ago. The short-term clinical performance was satisfactory so far.

All the same, certain limitations still exist in this study. The proposed method is based on the static loading conditions of six routine activities rather than dynamic, and the latter might provide more realistic physiological loading conditions. Muscles and ligaments were not included in the FEA model for simplification purposes due to their tiny effect on the stress magnitude. However, the presence of muscle forces will certainly distribute the stresses more evenly in the pelvis [33]. Moreover, the contact interfaces at sacroiliac joints, pubic symphysis and between bone and implant were modeled with tied (bonded) contact in order to increase the computational efficiency, thereby, sacrificing some accuracy with respect to the physiological environment. Furthermore, the results related to the optimized prostheses stability only rely on the FEA of the developed model and no mechanical test was performed. Additional mechanical tests to validate the FEA and strength of the optimized prostheses should be taken into account. In future studies, mechanical experiments will be conducted in order to probe the prosthetic strength.

5. Conclusion

A TO method for the designing of hemi-pelvic prostheses for various types of pelvic bone resections is proposed and applied. To incorporate the mechanical environments of various daily routine activities, a multi-load objective function has been formulated for the most occurring activities. Through this process, different hemi-pelvic implant designs were obtained, and the safety of the implant structures was validated through FEA. Following the TO method proposed in this article, a pelvic prosthesis for type II+III resection has been designed, manufactured and implanted, which shows good short-term clinical outcomes. In conclusion, the TO method developed in this study can provide a reasonable design of the pelvic prostheses for all types of resection, with optimized lightweight and strength guaranteed to be safe for all daily activities. This provides an effective design and functional evaluation tool for customized pelvic implants design before clinical application. Further efforts should contribute to improving the design using shape optimization and optimized design of the connecting part between the implants and the residue bone.

Declaration of conflicting interests

The author(s) declared no potential conflicts of interest with respect to the research, authorship and/or publication of this article.

Acknowledgments

The work was supported by National Key R&D Program of China [Grant number 2016YFC1100500 and 2018YFB1107000], Key Program of International Cooperation in Shaanxi Province [Grant number 2017KW-ZD-02] and the Fundamental Research Funds for the Central Universities.

Ethical approval

The ethical approval has been taken from the ethics committees of People's Hospital of Inner Mongolia, Neimenggu, China and Xijing Hospital Xi'an, China to use the CT data and postoperative images of the patients involved in this study.

Supplementary material

Supplementary material associated with this article can be found, in the online version, at doi:10.1016/j.medengphy.2019.06.008.

References

[1] Hugate R Jr, Sim FH. Pelvic reconstruction techniques. Orthop Clin North Am 2006;37:85–97. http://doi.10.1016/j.ocl.2005.08.006.
[2] Enneking WF, Dunham WK. Resection and reconstruction for primary neoplasms involving the innominate bone. J Bone Joint Surg Am 1978;60:731–46. https://doi.org/10.2106/00004623-197860060-00002.
[3] Zang J, Guo W, Yang Y, Xie L. Reconstruction of the hemipelvis with a modular prosthesis after resection of a primary malignant peri-acetabular tumour involving the sacroiliac joint. Bone Joint J 2014;96-B:399–405. http://doi.10.1302/0301-620X.96B3.32387.
[4] Liu D, Hua Z, Yan X, Jin Z. Design and biomechanical study of a novel adjustable hemipelvic prosthesis. Med Eng Phys 2016;38:1416–25. http://doi.10.1016/j.medengphy.2016.09.017.
[5] Singh VA, Elbahri H, Shanmugam R. Biomechanical analysis of a novel acetabulum reconstruction technique with acetabulum reconstruction cage and threaded rods after type II pelvic resections. Sarcoma 2016;2016:8627023. http://doi.10.1155/2016/8627023.
[6] Issa SP, Biau D, Babinet A, Dumaine V, Le Hanneur M, Anract P. Pelvic reconstructions following peri-acetabular bone tumour resections using a cementless ice-cream cone prosthesis with dual mobility cup. Int Orthop 2018;42:1987–97. http://doi.10.1007/s00264-018-3785-2.
[7] Fisher NE, Patton JT, Grimer RJ, Porter D, Jeys L, Tillman RM, et al. Ice-cream cone reconstruction of the pelvis: a new type of pelvic replacement: early results. J Bone Joint Surg Br 2011;93:684–8. http://doi.10.1302/0301-620X.93B5.25608.
[8] Aljassir F, Beadel GP, Turcotte RE, Griffin AM, Bell RS, Wunder JS, et al. Outcome after pelvic sarcoma resection reconstructed with saddle prosthesis. Clin Orthop Relat Res 2005;438:36–41. http://doi.10.1097/01.blo.0000179588.19479.34.
[9] Wang B, Xie X, Yin J, Zou C, Wang J, Huang G, et al. Reconstruction with modular hemipelvic endoprosthesis after pelvic tumor resection: a report of 50 consecutive cases. PLoS ONE 2015;10:e0127263. http://doi.10.1371/journal.pone.0127263.
[10] Arabnejad Khanoki S, Pasini D. Multiscale design and multiobjective optimization of orthopedic hip implants with functionally graded cellular material. J Biomech Eng Trans ASME 2012;134:031004. http://doi.10.1115/1.4006115.
[11] Kevin C, Joan E. Prosthetics and patient management: a comprehensive clinical approach. 1st ed. New Jersey: Slack Incorporated; 2006.
[12] Xiao D, Yang Y, Xu-bin S, Wang D, Luo Z. Topology optimization of microstructure and selective laser melting fabrication for metallic biomaterial scaffolds. T Nonferr Meta Soc 2012;22:2554–61. https://doi.org/10.1016/S10036326(11)615008.
[13] Kang H, Long JP, Urbiel Goldner GD, Goldstein SA, Hollister SJ. A paradigm for the development and evaluation of novel implant topologies for bone fixation: implant design and fabrication. J Biomech 2012;45:2241–7. http://doi.10.1016/j.jbiomech.2012.06.011.
[14] Yang XY, Xei YM, Steven GP, Querin OM. Bidirectional evolutionary method for stiffness optimization. AIAA J 1999;37:1483–8. https://doi.org/10.1016/10.2514/2.626.
[15] Melchels FPW, Domingos MAN, Klein TJ, Malda J, Bartolo PJ, Hutmacher DW. Additive manufacturing of tissues and organs. Prog Polym Sci 2012;37:1079–104. http://doi.10.1016/j.progpolymsci.2011.11.007.
[16] Fraldi M, Esposito L, Perrella G, Cutolo A, Cowin SC. Topological optimization in hip prosthesis design. Biomech Model Mechan 2010;9:389–402. http://doi.10.1007/s10237-009-0183-0.
[17] Kim BJ, Yun DK, Lee SH, Jang G-W. Topology optimization of industrial robots for system-level stiffness maximization by using part-level metamodels. Struct Multidiscip Optim 2016;54:1061–71. http://doi.10.1007/s00158-016-1446-x.
[18] Gao D, Wang D, Wang G, Hao L. Topology optimization of conditioner suspension for mower conditioner considering multiple loads. Math Comput Model 2013;58:489–96. http://doi.10.1016/j.mcm.2011.10.075.
[19] Chang CL, Chen CS, Huang CH, Hsu ML. Finite element analysis of the dental implant using a topology optimization method. Med Eng Phys 2012;34:999–1008. https://doi.org/10.1016/j.medengphy.2012.06.004.
[20] Sutradhar A, Park J, Carrau D, Nguyen TH, Miller MJ, Paulino GH. Designing patient-specific 3D printed craniofacial implants using a novel topology optimization method. Med Biol Eng Comput 2016;54:1123–35. http://doi.10.1007/s11517-015-1418-0.
[21] Yoon Y, Sun X, Huang J-K, Hou G, Rechowicz K, McKenzie FD. Designing natural-tooth-shaped dental implants based on soft-kill option optimization. Comput Aided Des Appl 2013;10:59–72. http://doi.10.3722/cadaps.2013.59-72.
[22] Zhong ZC, Wei SH, Wang JP, Feng CK, Chen CS, Yu CH. Finite element analysis of the lumbar spine with a new cage using a topology optimization method. Med Eng Phys 2006;28:90–8. http://doi.10.1016/j.medengphy.2005.03.007.
[23] Chuah HG, Abd Rahim I, Yusof MI. Topology optimisation of spinal interbody cage for reducing stress shielding effect. Comput Method Biomec 2010;13:319–26. http://doi.10.1080/10255840903208189.

[24] Andrade-Campos A, Ramos A, Simões JA. A model of bone adaptation as a topology optimization process with contact. J Biomedical Sci Eng 2012;05:229–44. http://doi.10.4236/jbise.2012.55030.
[25] Boyle C, Kim IY. Comparison of different hip prosthesis shapes considering micro-level bone remodeling and stress-shielding criteria using three-dimensional design space topology optimization. J Biomech 2011;44:1722–8. https://doi.org/10.1016/j.jbiomech.2011.03.038.
[26] Kharmanda G. Integration of multi-objective structural optimization into cementless hip prosthesis design: improved Austin-Moore model. Comput Method Biomec 2016;19:1557–66. http://doi.10.1080/10255842.2016.1170121.
[27] Ruben RB, Folgado J, Fernandes PR. Three-dimensional shape optimization of hip prostheses using a multicriteria formulation. Struct Multidiscip Optim 2007;34:261–75. http://doi.10.1007/s00158-006-0072-4.
[28] Saravana Kumar G, George SP. Optimization of custom cementless stem using finite element analysis and elastic modulus distribution for reducing stress-shielding effect. Proc Inst Mech Eng H 2017;231:149–59. https://doi.org/10.1177/0954411916686125.
[29] Wang X, Xu S, Zhou S, Xu W, Leary M, Choong P, et al. Topological design and additive manufacturing of porous metals for bone scaffolds and orthopaedic implants: a review. Biomaterials 2016;83:127–41. http://doi.10.1016/j.biomaterials.2016.01.012.
[30] Iqbal T, Shi L, Wang L, Liu Y, Li D, Qin M, et al. Development of finite element model for customized prostheses design for patient with pelvic bone tumor. Proc Inst Mech Eng H 2017;231:525–33. http://doi.10.1177/0954411917692009.
[31] Leung AS, Gordon LM, Skrinskas T, Szwedowski T, Whyne CM. Effects of bone density alterations on strain patterns in the pelvis: application of a finite element model. Proc Inst Mech Eng H 2009;223:965–79. http://doi.10.1243/09544119JEIM618.
[32] Bergmann G, Deuretzbacher G, Heller M, Graichen F, Rohlmann A, Strauss J, et al. Hip contact forces and gait patterns from routine activities. J Biomech 2001;34:859–71. https://doi.org/10.1016/S0021-9290(01)00040-9.
[33] Phillips ATM, Pankaj P, Howie CR, Usmani AS, Simpson AH. Finite element modelling of the pelvis: inclusion of muscular and ligamentous boundary conditions. Med Eng Phys 2007;29:739–48. http://doi.10.1016/j.medengphy.2006.08.010.
[34] Sigmund O. A 99 line topology optimization code written in matlab. Struct Multidiscip Optim 2001;21:120–7. http://doi.10.1007/s001580050176.
[35] Bendsøe MP, Sigmund O. Topology optimization theory, methods and applications. 1st ed. Berlin: Springer; 2002.
[36] Bendsøe MP, Sigmund O. Material interpolation schemes in topology optimization. Arch Appl Mech 1999;69:635–54. http://doi.10.1007/s004190050248.
[37] Guo W, Li D, Tang X, Yang Y, Ji T. Reconstruction with modular hemipelvic prostheses for periacetabular tumor. Clin Orthop Relat Res 2007;461:180–8. https://doi.org/10.1097/BLO.0b013e31806165d5.
[38] Liang H, Ji T, Zhang Y, Wang Y, Guo W. Reconstruction with 3D-printed pelvic endoprostheses after resection of a pelvic tumour. Bone Joint J 2017;99-B:267–75. http://doi.10.1302/0301-620X.99B2.BJJ-2016-0654.R1.
[39] Tao Z, Ahn HJ, Lian CL, Lee KH, Lee CH. Design and optimization of prosthetic foot by using polylactic acid 3D printing. J Mech Sci Technol 2017;31:2393–8. https://doi.org/10.1007/s12206-017-0436-2.
[40] Neumann DA. Kinesiology of the musculoskeletal system. 1st ed. St. Louis, Missouri: Mosby; 2010.
[41] Li Z, Kim JE, Davidson JS, Etheridge BS, Alonso JE, Eberhardt AW. Biomechanical response of the pubic symphysis in lateral pelvic impacts: a finite element study. J Biomech 2007;40:2758–66. http://doi.10.1016/j.jbiomech.2007.01.023.
[42] Tong J, Bowen CR, Persson J, Plummer A. Mechanical properties of titanium-based Ti–6Al–4V alloys manufactured by powder bed additive manufacture. Mater Sci Tech Ser 2016;33:138–48. http://doi.10.1080/02670836.2016.1172787.
[43] Vrancken B, Thijs L, Kruth J-P, Van Humbeeck J. Heat treatment of Ti6Al4V produced by selective laser melting: microstructure and mechanical properties. J Alloy Compd 2012;541:177–85. http://doi.10.1016/j.jallcom.2012.07.022.
[44] Wolff J. The internal architecture of normal bone and its mathematical significance. In: Wolff J, editor. The law of bone remodelling. Berlin: Springer; 1986. p. 3–22.